

Anisotropic Upper Critical Fields of Disordered $\text{Nb}_{0.53}\text{Ti}_{0.47}\text{-Ge}$ Multilayers

B. Y. Jin and J. B. Ketterson

Department of Physics and Astronomy and Materials Research Centre, Northwestern University,
Evanston, Illinois

E. J. McNiff, Jr. and S. Foner

Francis Bitter National Magnet Laboratory, MIT, Cambridge, Massachusetts

Ivan K. Schuller

Materials Science and Technology Division, Argonne National Laboratory, Argonne, Illinois

(Received March 24, 1987)

Studies are reported of the upper critical fields of $\text{Nb}_{0.53}\text{Ti}_{0.47}\text{-Ge}$ multilayers consisting of thick Ge layers and varying-thickness $\text{Nb}_{0.53}\text{Ti}_{0.47}$ layers. Both the angular dependence and the temperature dependence of the upper critical fields indicate a dimensional crossover at a $\text{Nb}_{0.53}\text{Ti}_{0.47}$ layer thickness near 200 Å. All the 2D samples display a cusplike upper critical field angular dependence with a sharper cusp for thinner $\text{Nb}_{0.53}\text{Ti}_{0.47}$ layers. The parallel upper critical fields are tentatively fitted with an expression combining the 2D field dependence of Rickayzen, the paramagnetic limiting behavior of Maki, and the disorder-related Coulomb interaction effects of Maekawa and Fukuyama. The perpendicular fields are fitted with the Maekawa, Ebisawa, and Fukuyama theory; better agreement is obtained for thinner $\text{Nb}_{0.53}\text{Ti}_{0.47}$ sublayers when the paramagnetic limiting effect is included.

1. INTRODUCTION

The anisotropy of the upper critical fields H_{c2} of layered superconductors has attracted much interest in recent years. Anisotropy in H_{c2} can arise from the properties of the individual layers¹⁻⁵ if they are well isolated by barriers, or it may reflect the coupling of the superconducting layers through the barriers. The coupling involves the Josephson effect for insulating barriers⁶⁻⁸ and the proximity effect for metallic barriers;^{9,10} the presence of magnetic moments in the barriers also has a pronounced effect.^{11,12} A

detailed theory exists for the Josephson coupled superlattice in the limit of a vanishing thickness for the superconducting layers,⁸ and the proximity coupled system has been examined recently.⁹ Two representative systems that have been studied experimentally are Nb-Ge⁸ and Nb-Cu¹⁰; both involve the “clean” superconductor Nb. However, additional phenomena can arise when studying a multilayered superconductor that consists of “dirty” superconductors or when the superconducting layers are made ultrathin. It is now generally recognized that disorder results in the appearance of various quantum effects, such as electron localization and Coulomb interaction, and that these will greatly influence T_c , H_{c2} , and J_c .¹³⁻¹⁷

The present paper is concerned with the highly anisotropic upper critical fields of superconducting Nb_{0.53}Ti_{0.47}-Ge multilayers with thick Ge layer barriers. Evidence for a dimensional crossover was observed at a Nb_{0.53}Ti_{0.47} layer thickness D_s near 200 Å, as revealed by the differing temperature dependence of the parallel upper critical fields $H_{c2\parallel}$ and a cusplike structure in the angular dependence of $H_{c2}(\theta)$.

A proper theory for $H_{c2\parallel}$ of a dirty, quasi-2D superconductor is not available. Therefore, we have (somewhat arbitrarily) combined various theoretical expressions that individually treat orbital, spin-orbit, and localization-interaction effects into a single expression in order to discuss our experimental data. We constructed a generalization of Rickayzen’s expression⁵ for a finite-thickness superconducting slab to account for paramagnetic limiting and T_c degradation due to weak localization and interaction effects,¹² which satisfactorily describes the H_{c2} temperature dependence for different samples.

The perpendicular critical field data, on the other hand, can be fitted with the theory of Maekawa *et al.*,¹⁴ with an improved fit if a paramagnetic limiting term is included.

2. SAMPLE PREPARATION AND CHARACTERIZATION

The Nb_{0.53}Ti_{0.47}-Ge samples were prepared by dc magnetron sputtering with a multisubstrate four-gun sputtering system.¹⁸ The layering was achieved by alternatively positioning the substrate above Nb_{0.53}Ti_{0.47} alloy and pure Ge targets, respectively. Typically 60 consecutive bilayers were deposited on an ~200°C sapphire substrate. The deposition parameters and the layer-thickness determination are described elsewhere.¹⁷ High-angle θ -2 θ diffractometer scans show a textured growth of the Nb_{0.53}Ti_{0.47} layers with the bcc (110) plane parallel to the substrate. The Ge is amorphous due to the low deposition temperature. The existence of distinct and intense low-angle diffraction peaks indicated good layering in the film normal direction (Fig. 1). The position and relative intensities of these low-angle

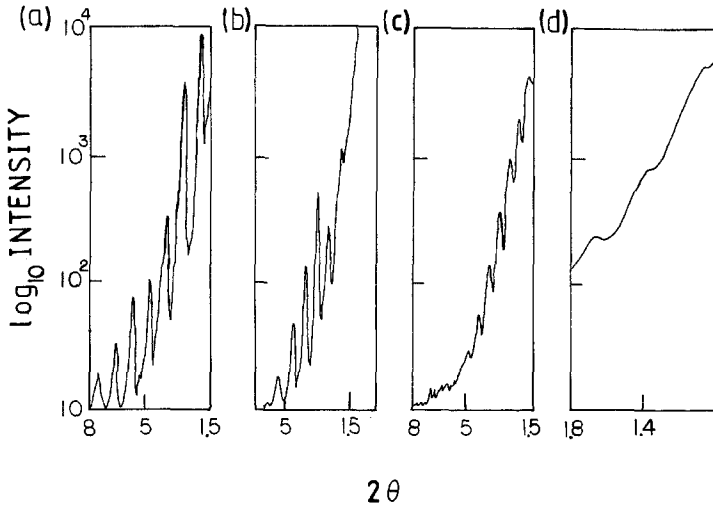


Fig. 1. Low-angle diffractometer scans of samples with Nb_{0.53}Ti_{0.47}/Ge ratio (a) 59 Å/38 Å, (b) 96 Å/45 Å, (c) 144 Å/32 Å, (d) 221 Å/45 Å.

peaks did not change noticeably in a period of 1 year, indicating very low room-temperature interlayer diffusion.

The upper critical field measurements were made in water-cooled magnets at the Francis Bitter National Magnet Laboratory. H_{c2} is defined as the midpoint of the resistance transition measured by a four-probe technique at a very low current level. The angular dependence of H_{c2} was measured with the multilayer structure mounted on a small, rotating support structure. For all the measurements the applied field was perpendicular to the current direction. Measurements at 4.2 K and below were made with the specimen in liquid He. Measurements above 4.2 K were made by placing the specimen in a temperature-controlled environment with the specimen in contact with He exchange gas.

3. RESULTS AND DISCUSSION

3.1. Parallel Upper Critical Fields $H_{c2\parallel}$

The $H_{c2\parallel}$ data on four samples are shown in Fig. 2. The lines are theoretical fits to the experimental data and will be explained later in this section. Table I lists the T_c , sheet resistance per layer R_{\square} , and other relevant parameters.

Figure 2 shows that the critical field "slope" $(dH_{c2\parallel}/dT)_{T=T_c}$ progressively increases for thinner D_s samples. The sample with the thickest D_s

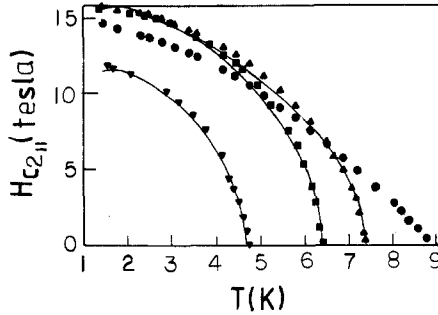


Fig. 2. Parallel upper critical fields of $\text{Nb}_{0.53}\text{Ti}_{0.47}/\text{Ge}$ samples: (▼) 59 Å/38 Å; (■), 96 Å/45 Å; (▲) 144 Å/32 Å; (●) 221 Å/45 Å. The lines are theoretical fits to the experimental data (see also Fig. 3).

exhibits a 3D-like behavior near T_c [$H_{c2||} \propto (1 - T/T_c)$], whereas the three remaining samples show a 2D-like behavior [$H_{c2||} \propto (1 - T/T_c)^{1/2}$]. These data clearly show that a dimensional crossover in the behavior of $H_{c2||}$ occurs near $D_s \approx 200$ Å.

Rickayzen has derived an expression suitable for thin films with $l \ll (\xi_0 l)^{1/2} \ll D_s$ which we employed in our earlier extrapolation of the zero-temperature critical field $H_{c2||}(0)$ from the behavior near T_c .¹⁷ The extrapolated values of $H_{c2||}(0)$ were several times larger than those experimentally

TABLE I
Sample Characteristics and Relevant Parameters^a

Sample	D_s (Å)/ D_{Ge} (Å)	T_c , K	R_{\square} , Ω
a	59/38	4.78	196
b	96/45	6.5	100
c	114/32	7.5	61
d	221/45	8.9	47

NbTi alloy:

Mean free path $l = 3.3$ Å

Fermi velocity (Nb)²⁰ $V_F \approx 2.6 \times 10^7$ cm/sec

BCS coherence length (Nb)^b $\xi_0 \approx 400$ Å

2D diffusion constant $D = \frac{1}{2} V_F l = 0.44$ cm²/sec

Spin-orbit scattering time¹ ($\text{Nb}_{0.44}\text{Ti}_{0.56}$) $\tau_{\text{so}} = 5.6 \times 10^{-14}$ sec

Exchange interaction strength¹⁷ $g_1 N(0) = 2$

^a D_s and D_{Ge} are the layer thicknesses of $\text{Nb}_{0.53}\text{Ti}_{0.47}$ and Ge, respectively.

^b The Nb value was used here for the BCS coherence length since precise Fermi velocity data are available for the pure metal; an appropriately defined alloy coherence length would not differ significantly.

determined here. The obvious reason (noted in ref. 17) for this overestimate is the neglect of the paramagnetic limiting affect at high fields.¹⁹ The paramagnetic limiting effect in a system with strong spin-orbit scattering usually enters as a separate term from the diamagnetic contribution to the upper critical fields.^{1,2,8} Here we assume that it is independent of the dimensionality. For lack of a complete theory, we have generalized the Rickayzen expression by arbitrarily introducing a paramagnetic limiting term into the argument of the ψ (digamma) function as follows:

$$\ln \frac{T}{T_{c0}} = \psi\left(\frac{1}{2}\right) - \text{av} \left\langle \psi\left(\frac{1}{2} + \frac{D\alpha^2}{4\pi k_B T} + \frac{3}{2} \frac{(\tau_{so}/\hbar)(\mu H)^2}{2\pi k_B T}\right) \right\rangle \quad (1)$$

where

$$\text{av} \langle F(z) \rangle = \frac{1}{D_s} \int_{-D_s/2}^{D_s/2} F(z) dz \quad (2)$$

Here T_{c0} is the superconducting temperature of a pure material, D is the diffusion constant, $\alpha^2 = \hbar(2ezH/\hbar c)^2$, μ is the Bohr magneton, and z is the spatial coordinate normal to the film plane. Due to the presence of disorder (as revealed by rapid decrease of T_c as the sheet resistance increases), we must model the effect of disorder on the upper critical fields by adding two Coulomb correction terms R_{HF} and R_V to the right-hand side of Eq. (7) and by modifying the diffusion constant.¹⁴ R_{HF} and R_V are terms calculated by Maskawa, Ebisawa, and Fukuyama (MEF)¹⁴ and arise from the Coulomb interaction contribution to the upper critical fields. The two terms are given by

$$R_{\text{HF}} = -\frac{\lambda_1}{2} K^2 - \lambda_1 K \left[\psi\left(\frac{1}{2}\right) - \psi\left(\frac{1}{2} + \frac{eDH_{c\perp}}{2\pi Tc}\right) \right] \quad (3)$$

$$R_V = -\frac{\lambda_1}{3} K^3 - \lambda_1 K^2 \left[\psi\left(\frac{1}{2}\right) - \psi\left(\frac{1}{2} + \frac{eDH_{c\perp}}{2\pi Tc}\right) \right] \quad (4)$$

where $K = \ln[5.4(\xi_0/l)T_{c0}/T]$. Here, $\lambda_1 = 1.25 \times 10^{-5} R_{\square} g_1 N(0)$, $g_1 N(0)$ is the exchange-interaction strength, and c is the speed of light. Equations (3) and (4) were derived for the perpendicular upper critical field.¹⁴ In the limit of a 2D system, only the vertical component of the magnetic field can enter the orbital effects in the interaction processes in the weakly localized regime.¹⁴ Therefore, only the first terms in Eqs. (3) and (4) were used in fitting the parallel upper critical fields. In the MEF theory, the diffusion constant is also modified by the localization effect. For a 2D system, the modified diffusion constant is given by¹⁴

$$D^* = D \left[1 - \lambda \ln\left(5.4 \frac{\xi_0}{l} \frac{T_{c0}}{T}\right) \right] \quad (5)$$

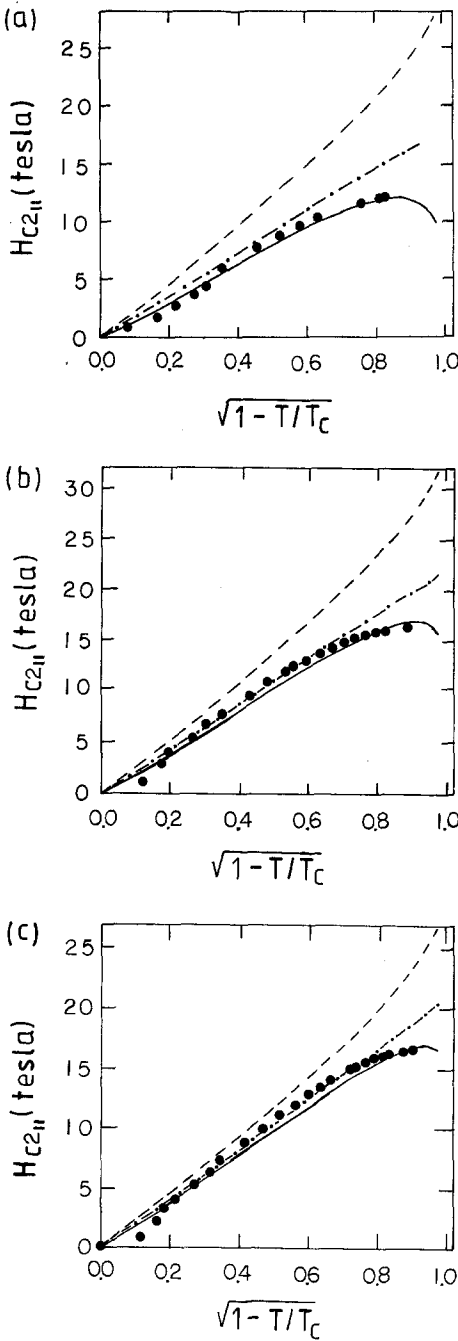


Fig. 3. Theoretical fit of $H_{c2||}$ as a function of $(1 - T/T_c)^{1/2}$ for the 2D samples. (---) From the Rickayzen theory, (-.-) from the Rickayzen theory with the paramagnetic limiting, (—) the generalized Rickayzen theory, which includes both the paramagnetic limiting and T_c degradation effects; (●) experimental data. The $\text{Nb}_{0.53}\text{Ti}_{0.47}\text{-Ge}$ thickness ratios ($D_s \text{ \AA}/D_{\text{Ge}} \text{ \AA}$) and the values of D_s (\AA) that best fit the data are as follows: (a) 59/38 and 90; (b) 96/45 and 96; (c) 144/32 and 124.

where $\lambda = 1.25 \times 10^{-5} R_{\square 9}$ and D^* should be substituted for D in Eq. (1). Finally, since the real T_c of the sample is degraded due to the localization effect, the quantity T_{c0} in Eq. (1) is replaced by the measured T_c by using the following expression¹³:

$$\ln \frac{T_{c0}}{T_c} = -\frac{\lambda_1}{2} \left[\ln \left(5.4 \frac{\xi_0}{l} \frac{T_{c0}}{T_c} \right) \right]^2 - \frac{\lambda_1}{3} \left[\ln \left(5.4 \frac{\xi_0}{l} \frac{T_{c0}}{T_c} \right) \right]^3 \quad (6)$$

Combining Eqs. (1) and (3)–(6), we obtained an expression for $H_{c2\parallel}$ as

$$\ln \frac{T}{T_c} = \psi \left(\frac{1}{2} \right) - \text{av} \left\langle \psi \left(\frac{1}{2} + \frac{D^* \alpha^2}{4\pi k_B T} + \frac{3}{2} \frac{(\tau_{so}/\hbar)(\mu H)^2}{2\pi k_B T} \right) \right\rangle - \frac{\lambda_1}{2} (K^2 - Q^2) - \frac{\lambda_1}{3} (K^3 - Q^3) \quad (7)$$

Here, $Q = \ln[5.4(\xi_0/l)T_{c0}/T_c]$. At $T = T_c$, $H_{c2} = 0$ and both sides of Eq. (7) vanish, as they should.

Equation (7) was solved numerically and fitted to the experimental data for the 2D samples. In Eq. (7), *all* parameters (see Table I) were either determined directly from zero-field experiments [T_c , $g_1 N(0)$,¹⁷ T_{c0} , R_{\square}] or estimated from other considerations (ξ_0 , l , v_F , D). For reasonable values for the latter parameters, the $H_{c2\parallel}(T)$ curve is completely determined by T_c and R_{\square} [note that $g_1 N(0)$ is obtained from the T_c versus R_{\square} curve, Eq. (6)]. We note that the same bulk spin-orbit scattering time τ_{so} was used for all samples. This is not generally legitimate due to some penetration of electrons into the Ge; however, it will be assumed that this effect does not significantly affect the analysis.

The results of the fitting with D_x as a free parameter are shown in Fig. 3 (D_x is the fitted Nb_{0.53}Ti_{0.47} layer thickness). The 2D theory does not fit a small region of the few low-field data near T_c . This could be due to a 3D to 2D crossover near T_c , some evidence for which is visible in the low-field data of Fig. 3. Note that the values that best fit the data for samples b and c are within 15% of the experimental values (D_s), which is consistent with the accuracy of the thickness determination. However, D_x for the sample with the thinnest D_s (59 Å) was 30 Å larger than the experimental value. It is not clear why such a large effective thickness is required for this sample, but it may relate to the spreading of the order parameter into the Ge layers.

3.2. Perpendicular Upper Critical Fields $H_{c2\perp}$

The perpendicular upper critical field $H_{c2\perp}$ of a disordered 2D superconductor has been studied theoretically by Maekawa, Ebisawa, and

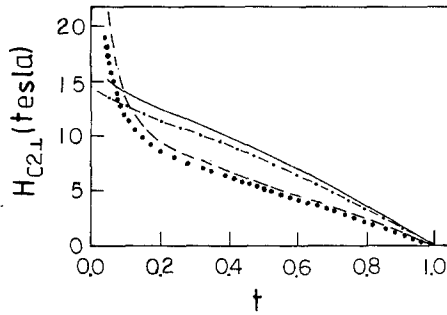


Fig. 4. Comparison of MEF theory with and without the inclusion of Pauli paramagnetic limiting. $t = T/T_c$ is the reduced temperature. MEF theory obtained with T_c and R_{\square} corresponding to samples with D_s/D_{Ge} equal to (---) 59 Å/38 Å and (—) 96 Å/45 Å; (-·-, ···) MEF theory with the inclusion of paramagnetic limiting.

Fukuyama¹⁴ (MEF). They obtained the following expression:

$$\ln \frac{T}{T_c} = \psi\left(\frac{1}{2}\right) - \psi\left(\frac{1}{2} + \frac{eD^*H}{2\pi k_B T_c}\right) + R_{HF} + R_V \quad (8)$$

The paramagnetic limiting term could be introduced here as in Eq. (1); however, this contribution is less important here than it is in the parallel field case in the temperature region studied, as can be seen from Fig. 4. The degraded T_c [determined with Eq. (6)] was again used here in place of T_{c0} . The experimental data and the theoretical curves are shown in

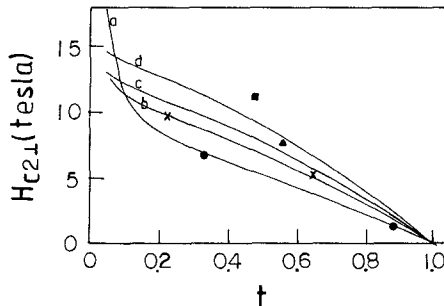


Fig. 5. Theoretical fit of the perpendicular upper critical fields as a function of reduced temperature $t = T/T_c$ with the MEF theory and paramagnetic limiting. The D_s/D_{Ge} values corresponding to each line and each symbol are: (a, ●) 59 Å/38 Å, (b, ×) 96 Å/45 Å, (c, ▲) 144 Å/32 Å, (d, ■) 221 Å/45 Å.

Fig. 5. We see from Fig. 5 that samples with thinner D_s fit the theory better, and also that the data for the 3D sample are in very poor agreement with the 2D theory, as would be expected. Here, the only two sample-dependent variables, T_c and R_{\square} , are determined from experiment. The fit is satisfactory and it is consistent with the T_c versus R_{\square} data [the same value $g_1 N(0) = 2$ was used for both]. Because only a few values $H_{c2\perp}$ were measured, the fitting of the perpendicular upper critical field here is only for the purpose of illustration.

3.3. The Angular Dependence of the Critical Fields

The angular dependence of the critical field $H_c(\theta)$ is shown in Fig. 6, where θ is the angle between the magnetic field and the film normal. We note that the sample with the thickest $\text{Nb}_{0.53}\text{Ti}_{0.47}$ layers ($D_s = 221 \text{ \AA}$) has essentially no anisotropy; it behaves as a bulk isotropic superconductor.

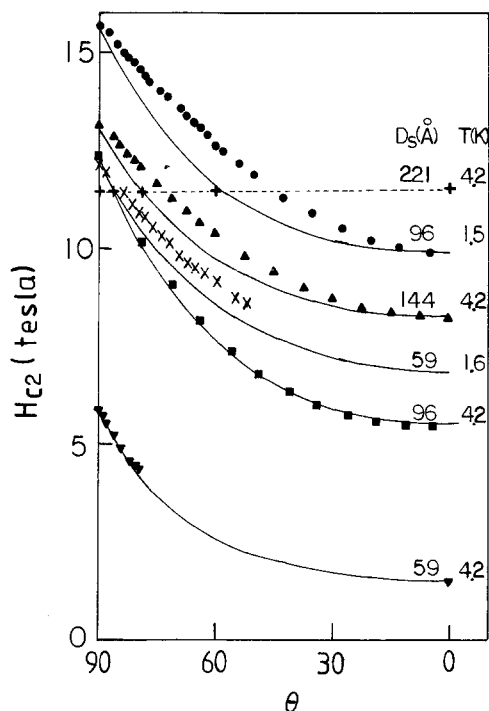


Fig. 6. Angular dependence of H_{c2} fitted with the Tinkham theory. (—) Theoretical predictions; (--) guidance for the eye; (▼) 59 Å/38 Å (4.2 K); (×) 59 Å/38 Å (1.6 K); (■) 96 Å/45 Å (4.2 K); (●) 96 Å/45 Å (1.5 K); (▲) 144 Å/32 Å (4.2 K); (+) 221 Å/45 Å (4.2 K).

The remaining three samples exhibit considerable anisotropy, and appear to display a cusp about the parallel field orientation.

For a bulk superconductor with uniaxial symmetry the angular dependence of the upper critical field $H_{c2}(\theta)$ is given by the so-called effective mass formula of Lawrence and Doniach⁶ (which follows from the Ginzburg-Landau theory)

$$\left[\frac{H_{c2}(\theta) \sin \theta}{H_{c2\parallel}} \right]^2 + \left[\frac{H_{c2}(\theta) \cos \theta}{H_{c2\perp}} \right]^2 = 1 \quad (9)$$

where $H_{c2\parallel} = \phi_0/2\pi\xi_{\parallel}\xi_{\perp}$, $H_{c2\perp} = \phi_0/2\pi\xi_{\parallel}^2$, ϕ_0 is the flux quantum, and ξ_{\parallel} and ξ_{\perp} are the in-plane and perpendicular coherence lengths, respectively. Equation (9) does not display a cusplike behavior and hence cannot apply directly to our data.

Tinkham²¹ has proposed the following expression for the angular dependence of the critical field for a thin film:

$$\left| \frac{H_{c2}(\theta) \cos \theta}{H_{c2\perp}} \right| + \left[\frac{H_{c2}(\theta) \sin \theta}{H_{c2\parallel}} \right]^2 = 1 \quad (10)$$

This expression does display a cusp and the solid line in Fig. 6 is obtained by fitting the parallel and perpendicular field measurements. For thinner samples and temperatures closer to T_c , the expression provides a good representation of the data.

We now discuss the applicability of Eq. (10) to our Josephson coupled metal/insulator superlattice. For those specimens that show a square root (2D)-like behavior of the temperature dependence of the upper critical field, it is reasonable to expect that each superconducting layer behaves as an isolated slab. For problems involving a magnetic field at an arbitrary angle with respect to either a slab or a semi-infinite sample, a separation of variables in a Ginzburg-Landau treatment is not possible. Minenko²² has treated the case of a superconducting slab of thickness D_s using a perturbation approach in the small parameter D_s/ξ_{\parallel} , where ξ_{\parallel} is the in-plane coherence length. His Eq. (23) may be written as

$$\left| \frac{2\pi\xi_{\parallel}^2}{\phi_0} H_c(\theta) \cos \theta \right| + \frac{(2\pi)^2 \xi_{\parallel}^2 D_s^2}{12\phi_0^2} H_c^2(\theta) \sin^2 \theta = 1 \quad (11)$$

This expression has the Tinkham form and reduces to the Lawrence-Doniach⁶ value for the field perpendicular to the slab, and to the Saint James-de Gennes²³ expression for the field parallel to the slab.

In superlattices with thick superconducting layers, or with strong Josephson coupling (thin Ge layers), a model involving a semi-infinite sample should apply. For the field parallel to the surface the phenomena

of surface superconductivity H_{c3} can be encountered. However, quite small currents are required to observe this effect. We note in passing that the angular dependence of $H_c(\theta)$ has been discussed by Yamafuji *et al.*²⁴ and Minenko.²²

The intermediate case involving the angular dependence of H_c when the Josephson coupling is neither large or small clearly requires further theoretical treatment.

4. CONCLUSIONS

We have extended earlier upper critical field measurements¹⁷ on Nb_{0.53}Ti_{0.47}-Ge multilayers to lower temperatures and higher magnetic fields. A dimensional crossover occurs at an Nb_{0.53}Ti_{0.47} layer thickness of ~ 200 Å. The parallel upper critical fields can be fitted by a Rickayzen-type formula only if paramagnetic limiting and the depression of T_c due to localization and interaction effects are included. The self-consistent fitting of $H_{c2\perp}$ and T_c versus R_{\square} provides a good test of the Maekawa *et al.*¹⁴ theory. We note that the WHH theory¹ with τ_{so} as a free parameter can also fit our parallel upper critical field data. The model expression fitted here accounts for the anisotropic upper critical fields, and the effects of "finite" layer thickness and the T_c degradation on the upper critical fields. It is worth mentioning that *all* the parameters (including τ_{so}) in our model were obtained from independent experiments or taken from the bulk values.

Josephson coupling was neglected in this paper, which presumes that the superconducting layers are well isolated by the thick Ge layers. The Josephson tunneling would certainly be important for multilayers with thinner barriers.⁸

Finally, a consistent theory is needed that includes the effects of orbital diamagnetism, spin-orbit coupling, spin paramagnetism, localization and interaction effects, finite film thickness, and the external field direction dependence.

ACKNOWLEDGMENTS

We would like to thank Dr. O. Fischer for helpful suggestions. This research was supported at Northwestern by the Materials Research Center under National Science Foundation grant DMR-82-16972, at the National Magnet Laboratory by NSF, and at Argonne National Laboratory under DOE BES-Materials Sciences grant W-31-109-ENG-38. One of us (B.Y.J.) would like to thank the IBM Corporation for the award of a postdoctoral fellowship.

REFERENCES

1. N. R. Werthamer, E. Helfand, and P. C. Hohenberg, *Phys. Rev.* **147**, 295 (1966).
2. K. Maki, *Phys. Rev.* **148**, 362 (1966).
3. Y. Nambu and S. F. Tuan, *Phys. Rev.* **133**, A1 (1964).
4. K. Maki, *Prog. Theor. Phys. (Kyoto)* **29**, 603 (1963).
5. G. Rickayzen, *Phys. Rev.* **138**, A73 (1965).
6. W. E. Lawrence and S. Doniach, in *Proceedings of the 12th International Conference on Low Temperature Physics*, E. Kanda, ed. (Academic Press of Japan, Kyoto, 1971), pp. 361-362.
7. G. Deutscher and O. E. Wohlman, *Phys. Rev. B* **17**, 1249 (1978).
8. R. A. Klemm, A. Luther, and M. R. Beasley, *Phys. Rev. B* **12**, 877 (1975); S. T. Ruggiero, T. W. Barbee, Jr., and M. R. Beasley, *Phys. Rev. Lett.* **45**, 1299 (1980).
9. M. Jochiki and S. Takahashi, in *Proceedings of the International Conference on Materials and Mechanisms of Superconductivity*. K. A. Gschneidner, Jr. and E. L. Wolf, eds. (North-Holland, Amsterdam, 1985).
10. C. S. L. Chun, G. G. Zheng, J. L. Vincent, and I. K. Schuller, *Phys. Rev. B* **29**, 4915 (1984).
11. P. W. Anderson and H. Suhl, *Phys. Rev.* **116**, 898 (1959).
12. H. K. Wong, B. Y. Jin, H. Q. Yang, J. B. Ketterson, and J. E. Hilliard, *J. Low Temp. Phys.* **63**, 307 (1986).
13. S. Maekawa and H. Fukuyama, *J. Phys. Soc. Jpn.* **51**, 1380 (1981).
14. S. Maekawa, H. Ebisawa, and H. Fukuyama, *J. Phys. Soc. Jpn.*, **52**, 1352 (1983); H. Fukuyama, private communications.
15. L. Coffey, K. A. Muttalib, and K. Levin, *Phys. Rev. Lett.* **52**, 783 (1984).
16. J. M. Graybeal and M. R. Beasley, *Phys. Rev. B* **29**, 4167 (1984).
17. B. Y. Jin, Y. H. Shen, H. K. Wong, J. E. Hilliard, J. B. Ketterson, and I. K. Schuller, *J. Appl. Phys.* **57**, 2543 (1985).
18. H. Q. Yang, B. Y. Jin, Y. H. Shen, H. K. Wong, J. E. Hilliard, and J. B. Ketterson, *Rev. Sci. Instr.* **56**, 607 (1985).
19. B. S. Chandrasekhar, *Appl. Phys. Lett.* **1**, 7 (1962); A. M. Clogston, *Phys. Rev. Lett.* **9**, 266 (1962).
20. G. W. Crabtree, D. H. Dye, D. P. Karim, and J. B. Ketterson, *Inst. Phys. Conf. Ser.* **39**, 683 (1978).
21. M. Tinkham, *Phys. Lett.* **9**, 217 (1964); F. E. Harper and M. Tinkham, *Phys. Rev.* **172**, 441 (1968).
22. E. V. Minenko, *Sov. J. Low Temp. Phys.* **9**, 535 (1983).
23. D. Saint James and P. G. de Gennes, *Phys. Lett.* **7**, 306 (1963).
24. K. Yamafuji, E. Kusayanagi, and F. Irie, *Phys. Lett.* **21**, 11 (1966).